

Fission fragment mass distribution in the $^{13}\text{C}+^{182}\text{W}$ and ^{176}Yb reactions

K. Ramachandran^{1,2,a}, D.J. Hinde^{1,b}, M. Dasgupta¹, E. Williams¹, A. Wakhle¹, D.H. Luong¹, M. Evers¹, I.P. Carter¹, and S. Das¹

¹Department of Nuclear Physics, The Australian National University, ACT 0200, Australia

²Permanent Address: Nuclear Physics Division, Bhabha Atomic Research Centre, Trombay, Mumbai 400085, India

Abstract. Shell effects can play a prominent role in fission fragment mass distributions. For lighter systems in the region of $A \sim 180$ -200, mass distributions were generally expected to be symmetric. However, a recent experiment showed that fission of ^{180}Hg following electron capture of ^{180}Tl leads to an asymmetric mass split. Recent calculations by various groups indicate that the mechanism of asymmetric fission could be very different in this mass region compared to the actinide region. To investigate the role of shell effects in this mass region, we have measured the fission fragment mass distribution for the $^{13}\text{C}+^{182}\text{W}, ^{176}\text{Yb}$ reactions forming the compound nuclei ^{195}Hg and ^{189}Os respectively, at lab bombarding energies of 60, 63 and 66 MeV using the CUBE detector setup located at the ANU Heavy Ion Accelerator Facility. The experimental data were fitted with single and double Gaussian distributions. The results indicate an asymmetric mass split for ^{195}Hg , whereas for ^{189}Os , the mass distribution is well fitted with a single Gaussian distribution.

1 Introduction

Nuclear fission is a dynamic process involving large scale shape changes. One important shape variable is the asymmetry between the volumes (masses) of the two fragments. Fission fragment mass distributions have been measured for many systems and found to be asymmetric in the fission of typical actinide nuclei for nucleon number A in the range 228-258 and proton number Z in the range 90-100. The mean mass of the heavy fragment remains constant at around 139 ± 1 and the mass of the light fragment increases linearly with the mass of the fissioning nucleus. The liquid drop model, which was reasonably successful in explaining the fission process, is unable to explain the mass distribution at lower energies for fission of nuclei in the mass region 228-258. Shell effects in the near scission configuration fragments were required to explain fission fragment mass distributions.

For lighter systems, it has been observed that fission fragment mass distributions are usually symmetric. It is difficult to measure fission fragment mass distributions at reasonably low excitation energy in such low fissility nuclei (in the mass region of 180-200). At high excitation energies the shell effects are expected to vanish and the nuclei are expected to behave like a charged liquid drop; hence, only symmetric fission is expected. Even after much experimental and theoretical work in this field, the rate of damping of shell effects with excitation energy is not well known.

The recent observation of asymmetric fission of ^{180}Hg following the electron-capture decay of ^{180}Tl [1] has triggered a lot of interest. This fission naturally occurs at a low excitation energy, and hence shell effects, if present, are expected to be observed in the fission fragment mass distribution. Calculations [1] showed that the potential energy surface (PES) for this nucleus has a deep symmetric valley at large deformation of the compound nucleus. Still, the nuclei were fissioning with an asymmetric mass split rather than a symmetric one. The reason given by the authors was as follows. The fissioning nuclei had an asymmetric trough in the PES at lower elongation along the fissioning axis, separated by a symmetric ridge which finally disappeared at high elongation. When the nuclei reached close to the symmetric valley in the PES, the neck of the fissioning nucleus had constricted so much that not much mass exchange could occur between the fragments towards the symmetric valley; hence, the mass degree of freedom was essentially frozen at that point. As a result, nuclei which were travelling through the asymmetric trough in the PES remained asymmetric until they fissioned. The centroid of the asymmetric mass peak is expected to be affected by the presumed small amount of mass exchange taking place at the later stage. This measurement [1], which had low compound nucleus excitation energy, showed the importance of dynamical effects in the fission process rather than the simple shell correction to the potential energy surface near scission in this mass region. There were also a few measurements in this mass region by M.G. Itkis *et al.* [2, 3] in the 1990s, which showed either a flat topped mass distribution or even a dip in the centre of the mass distribution. Further analysis of

^ae-mail: ramachandran.kandasamy@anu.edu.au

^be-mail: david.hinde@anu.edu.au

the same data by S.I. Mulgin [4] *et al.* suggested that the fission mass distribution may be affected by two deformed neutron shell closures at $N=52$ and 68 .

Following the measurement by A.N. Andreyev *et al.* [1], many theoretical calculations aimed at reproducing their observation were performed [5–8]. These calculations explained the data very well. There were also some preliminary predictions of an asymmetric mass split in the neutron rich W, Re, Os and Ir isotopes by P. Möller and J. Randrup [9] that seem to be influenced by the spherical doubly magic ^{132}Sn nuclei. The enhanced stability around ^{132}Sn is believed to play a role in the fission of actinide nuclei and also in a few of the heavy preactinide nuclei (fission mode Standard I according to the terminology of Brosa *et al.* [10]). The ^{201}Tl , ^{195}Au and ^{187}Ir nuclei did not show any such effects due to the ^{132}Sn shell closure [2, 4]. One important question to ask at this point is about the effect of the N/Z ratio: Is a particular combination of deformed/spherical shell structure of the fragments responsible for this effect? Calculations by P. Möller [5] *et al.* also indicate the importance of N/Z ratio on the fission fragment mass distribution. Their calculation has predicted a more asymmetric fission with increasing excitation energy for the very neutron deficient isotopes of mercury, namely ^{174}Hg and ^{176}Hg which is opposite to expectations, while the other not so neutron deficient isotopes were behaving normally. With this background, it is important to measure the mass distribution of various nuclei in this mass region. This paper reports our measurements with ^{13}C beams on ^{182}W and ^{176}Yb targets.

2 Experimental Details and Analysis

The experiment was performed using the Heavy Ion Accelerator Facility at Australian National University, Canberra, Australia. The experiments were performed with pulsed ^{13}C beams of 60, 63 and 66 MeV in energy, with a pulse separation of 106.7 ns. Thin ^{182}W and ^{176}Yb targets were used for the experiment to minimize the fragment energy loss in the target. The ^{182}W target was of thickness $25 \mu\text{g}/\text{cm}^2$ with a $15 \mu\text{g}/\text{cm}^2$ ^{nat}C backing, whereas the ^{176}Yb target was of thicknesses $74 \mu\text{g}/\text{cm}^2$ with a similar ^{nat}C backing. In experiments with fission of such low fissile nuclei, high Z target impurity of even a 1ppm level could be problematic at energies above the Coulomb barrier. To minimize any such contribution, the beam energies were chosen to be just above the Coulomb barrier for the target of interest but below the Coulomb barrier for the possible high Z impurity (^{232}Th , ^{238}U). We have used the CUBE detector setup (see fig.1) which consists of two large-area ($284 \text{ mm} \times 357 \text{ mm}$) position sensitive multi-wire proportional counters (MWPCs) mounted at a distance of 180 mm from the target center. The forward detector was at a scattering angle of 45° and backward detector was at 135° with respect to the beam. Both the detectors had an angular coverage of 77° . For each fission fragment entering the MWPCs, the timing, energy loss in the gas, and position information corresponding to X and Y were recorded. The master trigger was generated from the backward detector in order to minimize triggers due to elastic scattering.

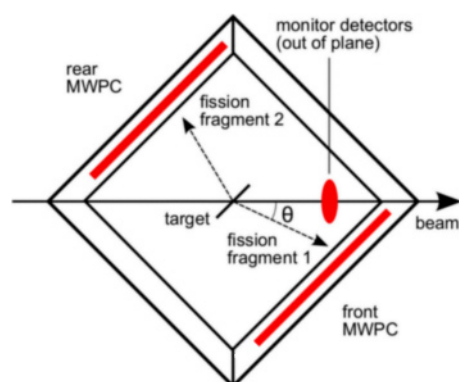


Figure 1. Configuration of the MWPCs for the detection of binary fission fragments

The fragment velocity vectors are determined using the position and timing information from the MWPCs. The mass ratio (M_R) is defined as:

$$M_R = M_2/(M_1 + M_2) = V_1/(V_1 + V_2), \quad (1)$$

where A_i (with $i=1,2$) represents the masses of each fragment i and V_i represents the center-of-mass velocity of each fission fragment. The above equation will not be valid if neutron evaporation changes the velocity of the fragment. In this event, some of the kinematic information is lost due to the undetected neutron. However, the isotropic nature of neutron emission means that the spread in the detected fragment velocity will increase while the average velocity will remain the same. Hence, with a good statistics the above equation should be applicable for calculating the mass ratios of the experimental data. While calculating the velocity of the fragments, energies of the fission fragments were corrected appropriately for energy loss in the target and backing; the beam energy was also corrected for energy loss in the target, assuming interactions occurred at half the target thickness. For pure compound nucleus fission, the average parallel component of the velocity is expected to be equal to the recoil velocity of the compound nucleus and the average velocity of the perpendicular component is expected to be zero. In the two reactions studied here, only compound nucleus fission is expected. Hence, a gate was applied on the 2D spectrum of parallel velocity versus the perpendicular velocity to exclude reactions with light impurities in the target and also to suppress random coincidences. Further details of the experimental setup and analysis procedure can be found in [11, 12].

The experimental mass ratio spectra for $^{13}\text{C}+^{182}\text{W} \rightarrow ^{195}\text{Hg}$ are shown in Fig. 2, 3 and 4. As can be seen from the figures, the $^{13}\text{C}+^{182}\text{W} \rightarrow ^{195}\text{Hg}$ fission shows signs of a flat topped mass distribution, similar to the experimental data for the nearby ^{195}Au nucleus [2]. The ^{195}Au data are at an excitation energy of around 10-11 MeV above the saddle point. With a fission barrier height of 18.8 MeV [13], the excitation energy above the saddle point ($E_{s.p.}^*$) for ^{195}Hg with angular momentum $0\hbar$ is 23.1 MeV at $E_{lab}=60 \text{ MeV}$ and 28.7 MeV at $E_{lab}=66 \text{ MeV}$ assuming

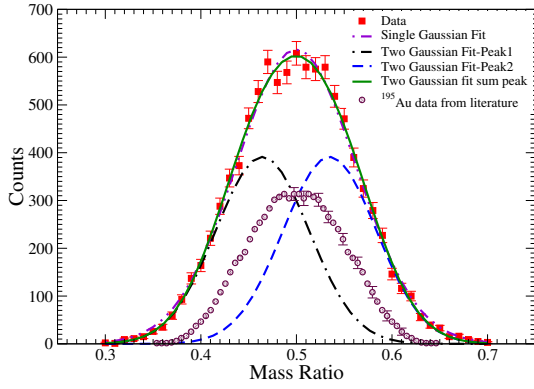


Figure 2. Fission fragment mass ratio distribution data along with single and double Gaussian fits for the $^{13}\text{C}+^{182}\text{W} \rightarrow ^{195}\text{Hg}$ system at $E^*_{g.s.}=47.5$ MeV. The ^{195}Au data from [2] also shown for comparison (see text).

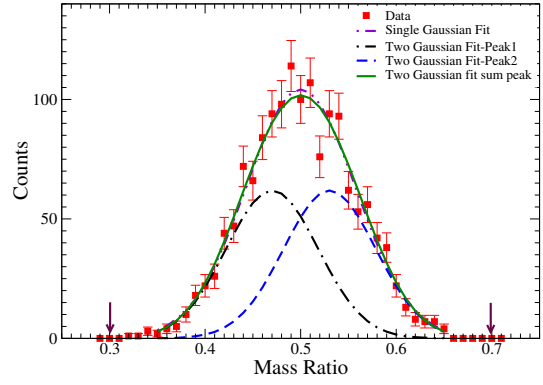


Figure 5. Fission fragment mass ratio distribution data along with single and double Gaussian fits for the $^{13}\text{C}+^{176}\text{Yb} \rightarrow ^{189}\text{Os}$ system at $E^*_{g.s.}=50.1$ MeV.

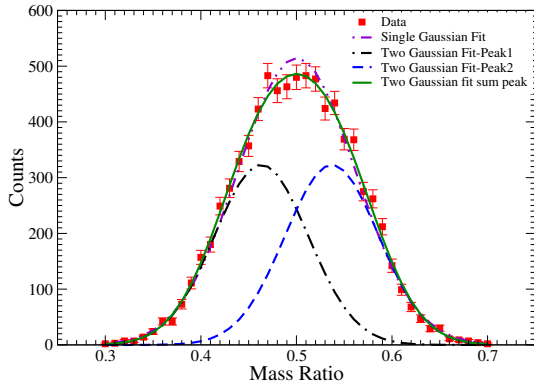


Figure 3. Fission fragment mass ratio distribution data along with single and double Gaussian fits for the $^{13}\text{C}+^{182}\text{W} \rightarrow ^{195}\text{Hg}$ system at $E^*_{g.s.}=44.7$ MeV.

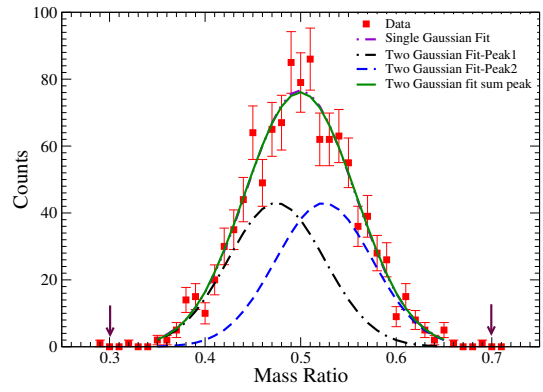


Figure 6. Fission fragment mass ratio distribution data along with single and double Gaussian fits for the $^{13}\text{C}+^{176}\text{Yb} \rightarrow ^{189}\text{Os}$ system at $E^*_{g.s.}=47.3$ MeV.

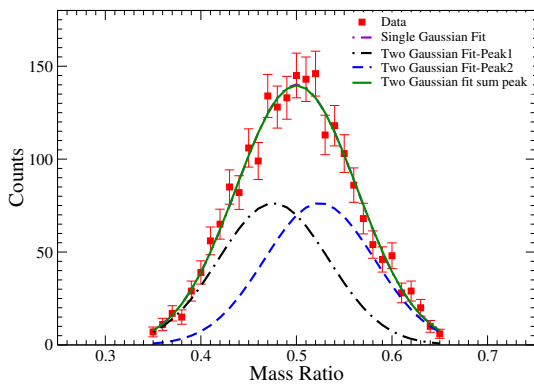


Figure 4. Fission fragment mass ratio distribution data along with single and double Gaussian fits for the $^{13}\text{C}+^{182}\text{W} \rightarrow ^{195}\text{Hg}$ system at $E^*_{g.s.}=41.9$ MeV.

there is no presaddle neutron evaporation. Due to the low fissility of ^{195}Hg , mostly first chance fission is expected; hence the assumption of no presaddle neutron evaporation is reasonable.

The mass ratio distributions are reasonably well described by a single Gaussian with centroid at 0.5. To check whether there are any mass asymmetric components in the spectra, we have also fitted the data with two Gaussians. The fitting was constrained to have the same width and area in both the peaks. Tables 1 and 2 provide the width of the mass ratio distribution, and the χ^2/DF with single and double Gaussian fits respectively. Data at the two highest energies with much better statistics are better explained by a two Gaussian fit rather than a single Gaussian fit. Table 3 shows the centroids of the double Gaussian fit for these two energies. Neglecting prescission neutron evaporation, these mass ratio centroids correspond to fission fragment mass numbers 91 and 104 for the light group and heavy group respectively. The light fragment mass is same as the mass for nuclei with semi-magic shell closure at $Z=40$ and $N=50$. The calculation by A.V. Andreev [6] *et al.* predicts a similar centroid for the mass distribution of the neighbouring ^{196}Hg isotope.

The experimental mass ratio spectra for $^{13}\text{C}+^{176}\text{Yb} \rightarrow ^{189}\text{Os}$ are shown in Fig.5 and 6. The mass distributions do not show any asymmetric feature. These mass distributions can be compared with mass distribution for ^{187}Ir [2] at $E^*_{s.p.}=10-11$ MeV which is the closest available mea-

Table 1. Single Gaussian fitting parameters for the mass ratio distribution

System	E*(MeV)	σ_m	χ^2/DF
$^{13}\text{C}+^{182}\text{W}$	41.9	0.0626±0.0013	0.69
$^{13}\text{C}+^{182}\text{W}$	44.7	0.0617±0.0004	1.57
$^{13}\text{C}+^{182}\text{W}$	47.5	0.0609±0.0004	1.12
$^{13}\text{C}+^{176}\text{Yb}$	47.3	0.0566±0.0013	0.85
$^{13}\text{C}+^{176}\text{Yb}$	50.1	0.0574±0.0013	1.00

Table 2. Double Gaussian fitting parameters for the mass ratio distribution

System	E*(MeV)	σ_m	χ^2/DF
$^{13}\text{C}+^{182}\text{W}$	41.9	0.0574±0.0106	0.71
$^{13}\text{C}+^{182}\text{W}$	44.7	0.0489±0.0013	0.94
$^{13}\text{C}+^{182}\text{W}$	47.5	0.0515±0.0013	0.95
$^{13}\text{C}+^{176}\text{Yb}$	47.3	0.0506±0.0077	0.88
$^{13}\text{C}+^{176}\text{Yb}$	50.1	0.0485±0.0038	1.01

Table 3. Centroids of fitted peaks with double Gaussian fitting

System	E*(MeV)	Centroid1	Centroid2
$^{13}\text{C}+^{182}\text{W}$	44.7	0.463±0.002	0.537±0.002
$^{13}\text{C}+^{182}\text{W}$	47.5	0.468±0.002	0.532±0.002

surement. If an asymmetric mass split were present for $^{13}\text{C}+^{176}\text{Yb} \rightarrow ^{189}\text{Os}$ with ^{132}Sn as the heavy fragment, it should be seen at the mass ratio of 0.698. The arrows in Fig. 5 and 6 indicate the corresponding mass ratio for the heavy fragments around ^{132}Sn and its complementary fragment. The $E^*_{s.p.}$ for ^{189}Os nucleus is also expected to be less than 30 MeV in our measurements. It is estimated that the yield of ^{132}Sn -like fragments in the mass distribution to be less than 0.1%. Tables 1 and 2 provide the width of the mass ratio distribution, and the χ^2/DF with single and double Gaussian fits respectively for $^{13}\text{C}+^{176}\text{Yb} \rightarrow ^{189}\text{Os}$. The mass ratio distributions are well described by a single Gaussian with centroid at 0.5. The double Gaussian fit doesn't give a significant improvement. Indeed, the χ^2/DF is worse as another fit parameter is introduced.

3 Summary and Conclusions

The fission fragment mass distribution has been measured for $^{13}\text{C}+^{182}\text{W}$ and ^{176}Yb systems using the CUBE detector. The $^{13}\text{C}+^{182}\text{W} \rightarrow ^{195}\text{Hg}$ fission show flat topped mass distribution as might be expected. The experimental data were fitted with single and double Gaussians to understand the nature of the mass split for all energies. For $^{13}\text{C}+^{182}\text{W}$ system at the two highest excitation energies, the two Gaussian fit better represents the data, and at the lowest excitation energy, there is not a significant difference in the quality of fit between single and double Gaussian fits due to poor statistics. The centroid of the mass distribution peaks at around 91 mass units for the lighter frag-

ment and at around 104 mass units for the heavy fragment. It is interesting to note that the light mass group is close to the Z=40 and N=50 semi-magic shell closure. For the $^{13}\text{C}+^{176}\text{Yb}$ system, the single Gaussian has a marginally better χ^2/DF . The $^{13}\text{C}+^{176}\text{Yb} \rightarrow ^{189}\text{Os}$ fission does not show any asymmetric features, specifically no evidence for an asymmetric fission mode influenced by the doubly magic ^{132}Sn fragment. It will be interesting to calculate the PES for these two systems and perform dynamical model calculation to understand the mass distribution.

Acknowledgements

This work was supported by ARC grant DP110102858.

References

- [1] A.N. Andreyev, J. Elseviers, M. Huyse, P. Van Duppen, S. Antalic, A. Barzakh, N. Bree, T.E. Cocolios, V.F. Comas, J. Diriken et al., Phys. Rev. Lett. **105**, 252502 (2010)
- [2] M.G. Itkis, N.A. Kondratev, S.I. Mulgin, V.N. Okolovich, A.Y. Rusanov, G.N. Smirenkin, Sov. J. Nucl. Phys. **52**, 601 (1990)
- [3] M.G. Itkis, N.A. Kondratev, S.I. Mulgin, V.N. Okolovich, A.Y. Rusanov, G.N. Smirenkin, Sov. J. Nucl. Phys. **53**, 757 (1991)
- [4] S.I. Mulgin, K.H. Schmidt, A. Grewe, S.V. Zhadanov, Nucl. Phys. **A640**, 375 (1998)
- [5] P. Möller, J. Randrup, A.J. Sierk, Phys. Rev. C **85**, 024306 (2012)
- [6] A.V. Andreev, G.G. Adamian, N.V. Antonenko, Phys. Rev. C **86**, 044315 (2012)
- [7] T. Ichikawa, A. Iwamoto, P. Möller, A.J. Sierk, Phys. Rev. C **86**, 024610 (2012)
- [8] M. Warda, A. Staszczak, W. Nazarewicz, Phys. Rev. C **86**, 024601 (2012)
- [9] P. Möller, (*A*)symmetry of Fission in the $74 \leq Z \leq 90$, $A \leq 205$ Region, in *5th ASRC International Workshop "Perspectives in Nuclear Fission"* (JAEA, Tokai, Japan, Tokai, Japan, 2012)
- [10] U. Brosa, S. Grossmann, A. Müller, Phys. Rep. **197**, 167 (1990)
- [11] D.J. Hinde, M. Dasgupta, J.R. Leigh, J.C. Mein, C.R. Morton, J.O. Newton, H. Timmers, Phys. Rev. C **53**, 1290 (1996)
- [12] R.G. Thomas, D.J. Hinde, D. Duniec, F. Zenke, M. Dasgupta, M.L. Brown, M. Evers, L.R. Gasques, M.D. Rodriguez, A. Diaz-Torres, Phys. Rev. C **77**, 034610 (2008)
- [13] P. Möller, A.J. Sierk, T. Ichikawa, A. Iwamoto, R. Bengtsson, H. Uhrenholt, S. Åberg, Phys. Rev. C **79**, 064304 (2009)